NEOPLASIA
www.neoplasia.com

Volume 19 Number 1 January 2017 pp. 35–42 35

In Vitro and *In Vivo* Activity of Lucitanib in FGFR1/2 Amplified or Mutated Cancer Models[1,2]

Federica Guffanti[*,3], Rosaria Chilà[*,3], Ezia Bello[*], Massimo Zucchetti[†], Monique Zangarini[†], Laura Ceriani[†], Mariella Ferrari[†], Monica Lupi[†], Anne Jacquet-Bescond[‡], Mike F. Burbridge[‡], Marie-Jeanne Pierrat[‡] and Giovanna Damia[*]

[*]Laboratory of Molecular Pharmacology, Department of Oncology, IRCCS-Istituto di Ricerche Farmacologiche "Mario Negri", Via La Masa 19, 20156, Milan, Italy; [†]Laboratory of Cancer Pharmacology, Department of Oncology, IRCCS-Istituto di Ricerche Farmacologiche "Mario Negri", Via La Masa 19, 20156, Milan, Italy [‡]Servier Oncology R&D, 50 rue Carnot, 92284 Suresnes, Cedex, France

Abstract

The fibroblast growth factor receptor (FGFR) pathway has been implicated both as an escape mechanism from anti-angiogenic therapy and as a driver oncogene in different tumor types. Lucitanib is a small molecule inhibitor of vascular endothelial growth factor (VEGF) receptors 1 to 3 (VEGFR1 to 3), platelet derived growth factor α/β (PDGFRα/β) and FGFR1–3 tyrosine kinases and has demonstrated activity in a phase I/II clinical study, with objective RECIST responses in breast cancer patients with *FGFR1* or *FGF3/4/19* gene amplification, as well as in patients anticipated to benefit from anti-angiogenic agents. We report here the *in vitro* and *in vivo* antitumor activity of lucitanib in experimental models with or without *FGFR1/2* amplification or mutations. In cell assays, lucitanib potently inhibited the growth of tumor cell lines with amplified *FGFR1* or mutated/amplified *FGFR2*. In all xenograft models studied, lucitanib demonstrated marked tumor growth inhibition due to potent inhibition of angiogenesis. Notably, in two lung cancer models with *FGFR1* amplification, the antitumor efficacy was higher, suggesting that the simultaneous inhibition of VEGF and FGF receptors in *FGFR1* dependent tumors can be therapeutically advantageous. Similar antitumor activity was observed in *FGFR2* wild-type and amplified or mutated xenograft models. Pharmacokinetic studies showed lucitanib plasma concentrations in the micro/sub-micromolar range demonstrated drug accumulation following repeated lucitanib administration.

Neoplasia (2017) 19, 35–42

Introduction

Fibroblast growth factor receptors (FGFRs) play several roles in the control of cell proliferation, cell differentiation, angiogenesis, development and survival [1]. While the FGFR pathway was initially studied as a promoter of tumor angiogenesis with synergistic effects on the vascular endothelial growth pathway [2], recent studies have suggested that the pathway is involved both as an escape mechanism from anti-angiogenic therapy [3] and as a driving oncogene in certain tumors [4,5]. De-regulation of the FGFR pathway has been shown to induce tumor cell growth and to maintain the malignant properties of cancer cells. Alterations of the FGFR pathway in cancer include: gene amplification with receptor over-expression, *FGFR* mutations with

Address all correspondence to: Giovanna Damia, Department of Oncology, IRCCS-Istituto di Ricerche Farmacologiche "Mario Negri", Via La Masa 19, 20156, Milan, Italy.
E-mail: giovanna.damia@marionegri.it

[1] Financial support. This research was supported by a research grant from Servier.
[2] Conflict of interest: The authors declare that they have no conflict of interests.
[3] These authors equally contributed.
Received 19 October 2016; Revised 7 November 2016; Accepted 7 November 2016

1476-5586
http://dx.doi.org/10.1016/j.neo.2016.11.008

constitutive active receptor or reduced dependency on ligand binding, translocation to produce FGFR fusion proteins with constitutive kinase activity, alternative FGFR splicing leading to a different but broader ligand specificity and up-regulation of the FGF expression with subsequent paracrine/autocrine activation of the pathway [6–8]. The dependency on FGFR pathway has been reported in different human malignancies [9,10]. Amplification of *FGFR1* has been reported in breast cancers (~10%) [11,12], ovarian cancers (5%), lung squamous cell carcinomas (~20%) and lung adenocarcinomas (~3.5%) [13–15]. Approximately 5% of gastric cancers have been reported to bear *FGFR2* amplification [16]. *FGFR2* mutations occurs in about 12% of endometrial carcinoma. Up to 80% of low-grade and 20% of high grade bladder cancer harbor activating mutations in *FGFR3* [17,18].

The inhibition of the aberrant FGFR pathway in cancer models by anti-FGFR antibodies and/or small molecules has been shown to have robust antitumor effect [4]. Several multitarget tyrosine kinase inhibitors in clinical development, originally identified as ATP competitors of the vascular endothelial growth factor receptor (VEGFR) family, have been shown to have activity against one or more FGFRs in preclinical models (for an updated review see (4)): nintedanib [19] brivanib [20], dovitinib [21,22] and ponatinib [23]. Recently, more specific FGFR inhibitors lacking significant activity against VEGFR have been synthesized and are under clinical investigation: AZD4547 [24,25], LY2874455 [26], NVP-BGJ398 [22,23,27] and JNJ-42756493 [28].

Lucitanib is a novel small molecule that selectively binds VEGFR1-3, PDGFRα/β and FGFR1-3 tyrosine kinases in biochemical assays with Kd <100 nM [29]. The phase I/II clinical study of lucitanib demonstrated 4 confirmed and 2 unconfirmed objective RECIST responses among 12 breast cancer patients with FGF-aberrant (*FGFR1* and/or *FGF3/4/19* gene amplified) tumors. Objective RECIST responses were also observed in patients anticipated to benefit from antiangiogenic agents (e.g., renal cell carcinoma and thyroid cancer patients) [30].

We report here the *in vitro* and *in vivo* anti-FGFR activity of lucitanib using a panel of cell lines with aberrant or wild-type (wt) FGFR1-2 pathway. In addition, a comprehensive pharmacokinetic profile of the drug in *in vivo* models is presented.

Materials and Methods

Cell Lines and Drug Treatment

Ten non-small cell lung cancer (NSCLC) cell lines (H1299, H1975, H2342, H1650, H358, A549, H2228, H23, H1581, H520), one small cell lung cancer (SCLC) cell line (DMS114), three gastric (KATOIII, SNU16, MNK45) and three endometrial (HEC1A, MFE296, AN3CA) cancer cell lines were maintained in RPMI supplemented with 1% glutamine and 10% fetal bovine serum (FBS). Human umbelical vein cells (HUVEC) were maintained as monolayer in MCDB131 medium supplemented with 20% (v/v) FBS, 1% (v/v) L-glutamine, 5 Units/ml Heparin and 50 μg/ml endothelial cell growth factor (ECGF) using culture flasks or plates pre-coated with 1% (v/v) gelatine. All cell lines were obtained from the American Type Culture Collection and their authentication was carried out by the authors within the last 6 months.

Lucitanib was dissolved in DMSO in a stock solution of 10 mM and stored at −20 °C. All cell lines were treated with a range (0.01 to 50 μM) of lucitanib concentrations in 96-well plates 48 hours after seeding. A cell viability assay (CellTiter MTS, Promega, Italy) was performed 72 hours after treatment. Quantitation of fluorescence was measured at 490 nm in a microplate reader (Infinite M200, TECAN) after 2 hours of incubation with MTS ((3-(4,5-dimethylthiazol-2-yl)-5-(3-carboxymethoxyphenyl)-2-(4-sulfophenyl)-2H–tetrazolium) according to manufacturer's instruction. The efficacy of the treatment (half maximal inhibitory concentration, IC_{50}) was calculated by CalcuSyn Software (Biosoft, Cambridge, UK).

Molecular Analyses

DNA from lung cancer cell lines was extracted using the Maxwell 16 Cell DNA Purification Kit (Promega, Milan, Italy). The *FGFR1* and *FGFR2* gene copy numbers were assessed using a TaqMan Copy Number assay (no Hs00241111 and Hs01552926 respectively, Applied Biosystems, Monza, Milan). *RNAseP* copy number was used as reference gene. The PCR was carried out in 96-well plates with a reaction volume of 15 μL containing 10 ng of DNA, TaqMan Genotyping Master Mix (Applied Biosystems), primers and probes specifically designed for copy number analysis (Applied Biosystems). Thermal cycle conditions were 95°C for 10 minutes and 40 cycles of 95°C for 15 seconds and 60°C for 1 minute. Data were analyzed using the Copy Caller 2.0 Software (Applied Biosystems).

Real Time (RT)-PCR was used for relative quantification of *FGFR1*, *FGFR2* and *FGF2* mRNA. Total RNA from human umbilical vein/vascular endothelium HUVEC and lung cancer cell lines was purified with the SV40 Total RNA Isolation System (Promega) and reverse transcribed with the cDNA Archive Kit (Applied Biosystems). *FGFR1*, *FGFR2*, *FGF2*, and *ACTB* expression was detected using TaqMan assays (Applied Biosystems). Reactions were run in a total volume of 20 μL containing 8 ng of cDNA with TaqMan PCR Master Mix, following the manufacturer's instructions (Applied Biosystems). All the data were normalized to ACTB, and data are expressed as fold increase over the normalized value of HUVEC cells.

Two-Parameter Flow Cytometry Analysis: DNA Content and FITC-Conjugated dUTP

DNA fragmentation during apoptosis was detected by the TdT-mediated dUTP nick-end labeling technique (TUNEL), which uses terminal deoxynucleotidyl transferase (TdT) to catalyze the binding of FITC-conjugated dUTP to DNA strand breaks. DMS114 and H1299 cells treated either with DMSO or with the corresponding lucitanib IC_{50} doses, were fixed at different time points after treatment, washed in PBS and permeabilized for 2 minutes on ice in 0.1% Triton X-100, 0.1% sodium citrate. The cells were washed, re-suspended in 50 μL of TUNEL reaction mixture (Roche, Mannheim, Germany) containing dUTP-FITC and TdT, and incubated for 90 minutes at 37 °C in the dark. After that, the samples were washed and re-suspended in 1 μg/ml propidium iodide plus 25 μL of 1 mg/ml RNAse in water and incubated overnight at 4 °C.

Western Blotting

Protein extraction and Western Blot were performed as previously described [31]. Anti-Phospho(Y653/654)-panFGFR, anti-FGFR1, anti-FGFR2, anti-Phospho(Y436)FRS2, anti-Phospho(T202/Y204)ERK1/2 and anti-ERK1/2 antibodies were purchased from Cell Signaling (Danvers, MA), while anti-FRS2 antibody was purchased from R&D systems (Minneapolis, MN). Secondary anti-rabbit and anti-sheep

Table 1. Molecular Characteristics of the Cancer Cell Lines

Cell Line	Type	Gene Copy Number		mRNA			Mutational Status		
		FGFR1	FGFR2	FGFR1	FGFR2	FGF2	FGFR2	KRAS	TP53
H1299	NSCLC	1	2	0,58	0,90	3,79	wt	wt	wt
H1975	NSCLC	1	1	0,05	1,56	Undetermined	wt	wt	R273H
H2342	NSCLC	1	1	0,02	2484,32	0,09	wt	wt	Y220C
H1650	NSCLC	2	4	0,14	418,31	6,27	wt	wt	na
H358	NSCLC	1	1	0,01	72,74	Undetermined	wt	G12C	wt
A549	NSCLC	2	2	0,86	16,28	4,35	wt	G12S	wt
H2228	NSCLC	2	1	0,59	0,81	8,64	wt	wt	Q331*
H23	NSCLC	1	1	0,18	20,24	0,60	wt	G12C	M246I
H1581	NSCLC	4	2	2,37	2747,53	0,05	wt	wt	Q144*
H520	NSCLC	4	1	6,39	3,73	1,20	wt	wt	W146*
DMS114	NSCLC	5	3	6,37	36,30	4,33	wt	wt	R213*
HEC1A	Endometrial	2	4	0,33	544	Undetermined	wt	hetero G12D	G743A
MFE296	Endometrial	2	2	3	2771	16	N549K	wt	C916, A659G
AN3CA	Endometrial	2	3	22	6725	8995	N549K, K310R	wt	G1165 T, 267delC, G638A
MNK45	Gastric	1	2	0,16	475	0,067	wt	na	wt
SNU16	Gastric	2	>100	Undetermined	35,464	Undetermined	wt	wt	Y205F
KATO III	Gastric	2	>100	Undetermined	9236	Undetermined	wt	na	deleted

Gene copy number and mRNA expression levels were determined as described in Material and Methods. Mutational status derived from Cosmic database (http://cancer.sanger.ac.uk/cosmic).
wt, wild type; mut, mutated; na: not available.

HRP-conjugated antibodies were from Cell Signaling and Santa-Cruz Bio-technology (Santa-Cruz, *CA*) respectively.

Xenograft Models

Female NCr-nu/nu mice (6 weeks old) were obtained from ENVIGO RMS srl (Correzzana, Italy). They were maintained under specific pathogen free conditions, housed in isolated vented cages, and handled using aseptic procedures. The IRCCS-Istituto di Ricerche Farmacologiche Mario Negri adheres to the principles set out in the following laws, regulations, and policies governing the care and use of laboratory animals: Italian Governing Law (D. lg 26/2014; Authorization n.19/2008-A issued March 6, 2008 by Ministry of Health); Mario Negri Institutional Regulations and Policies providing internal authorization for persons conducting animal experiments (Quality Management System Certificate – UNI EN ISO 9001:2008 – Reg, No.6121); the NIH Guide for the Care and Use of Laboratory Animals (2011 edition) and EU directives and guidelines (EEC Council Directive 2010/63/UE). The Statement of Compliance (Assurance) with the Public Health Service (PHS) Policy on Human Care and Use of Laboratory Animals was recently reviewed (9/9/2014) and will expire on September 30, 2019 (Animal Welfare Assurance #A5023–01). H1581, DMS114, H1299, MFE296, SNU16, MNK45 and HEC1A tumors were subcutaneously transplanted into the flanks of nude mice as fragments. Mice were randomized when the average tumor size was 200–250 mm^3 (n = 8–10 per group), to receive lucitanib given orally at the dose of 2.5, 5, 10 or 20 mg/kg daily or vehicle (Methocel 0.5%) for 30 days. Tumor growth was measured twice weekly with a Vernier caliper, and the tumor volumes (mm^3) were calculated as follows: (length [mm] × width $[mm]^2$)/2. Tumor growth data were expressed as the mean ± SEM. Treatment efficacy was expressed as best tumor growth inhibition [%T/C = (median volume of treated tumors/median volume of control tumors) × 100]. Animals were euthanized when primary tumor volume exceeded 10% of body weight, evaluated the same day.

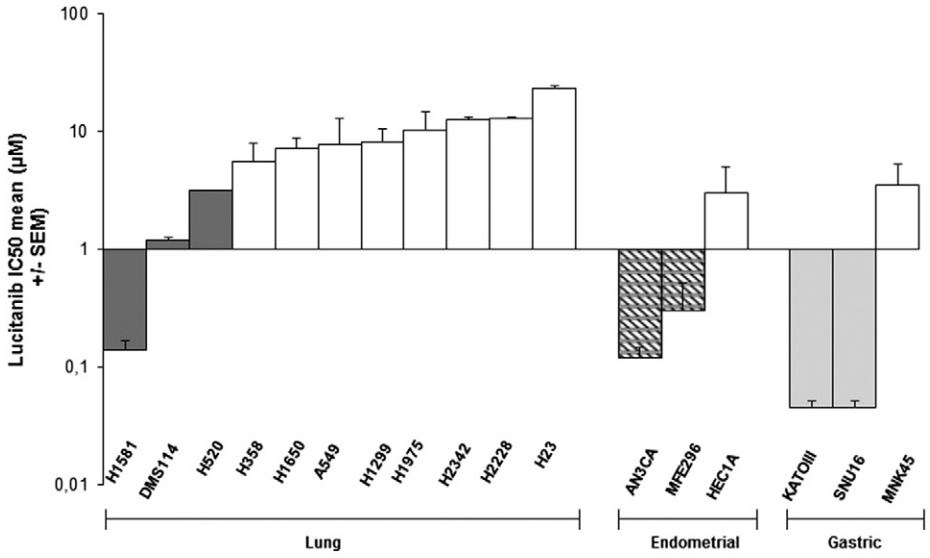

Figure 1. Lucitanib *in vitro* activity (IC_{50}) in lung, endometrial and gastric cancer cell lines. wt *FGFR1/2:* (□); amplified *FGFR1:*(■); amplified *FGFR2:* (■); mutated *FGFR2:* (□). IC_{50} values have been calculated as described in Materials and Methods and are the arithmetic mean IC_{50} (μM) + SEM.

Lucitanib Pharmacokinetics

Pharmacokinetic sampling was performed after 12 daily repeated lucitanib oral administrations (qdx12) in different xenograft models at several time intervals after dosing. Blood samples were collected at 4 and 24 hours post-dose for H1299 and DMS114 tumor bearing mice receiving daily doses of 2.5, 5, 10 and 20 mg/kg. Blood samples were collected at 4 hours and 24 hours post-dose for H1581 tumor bearing mice treated at 2.5, 5, 10 and 20 mg/kg daily doses and specifically for the 5 and 20 mg/kg doses, additional samplings were performed at 1, 2, and 8 hours post-treatment. Three to four mice were used per time-point; animals were anesthetized with isoflurane, blood was drawn into heparinized tubes from the retro-orbital plexus, centrifuged 10 min at 4000 rpm at 4 °C and plasma was separated and stored frozen at −20 °C. Mice were sacrificed by cervical dislocation and tumor samples were removed, snap-frozen and stored at −20 °C. Plasma and tumor concentrations of lucitanib after repeated oral doses were measured by LC–MS/MS analysis, as previously reported [32,33]. The lower limit of quantification of the method was 2 and 5 ng/ml lucitanib in plasma and tumors, respectively. The tumor-to-plasma lucitanib concentration ratio was calculated in mice sacrificed at 4 and 24 hours post-dosing. Data are expressed as μM concentration (mean ± standard deviation).

Results

FGFR1 Amplified or FGFR2 Amplified or FGFR2 Mutated Cancer Cell lines are Preferentially Sensitive to Lucitanib In Vitro

The present studies were undertaken to investigate lucitanib cytostatic/cytotoxic activity in *FGFR1/2* deregulated cell lines. A panel of 17 cancer cell lines (11 lung, 3 endometrial, and 3 gastric cancer cell lines) was characterized for *FGFR1/2* gene copy number, *FGFR1/2* and *FGF2* mRNA levels and mutational status of *FGFR2*, *TP53* and *KRAS* (Table 1). Gene amplification was defined positive when the gene copy number was higher or equal to 4. All *FGFR1* amplified lung cancer cell lines (DMS114, H1581, H520) overexpressed *FGFR1* mRNA (Table 1). On the contrary, *FGFR1* non-amplified lung cancer cell lines did not overexpress *FGFR1* mRNA. *FGFR1* mRNA fold increase correlated with *FGFR1* gene copy number (Supplementary Figure 1*A*). *FGFR1* amplified and

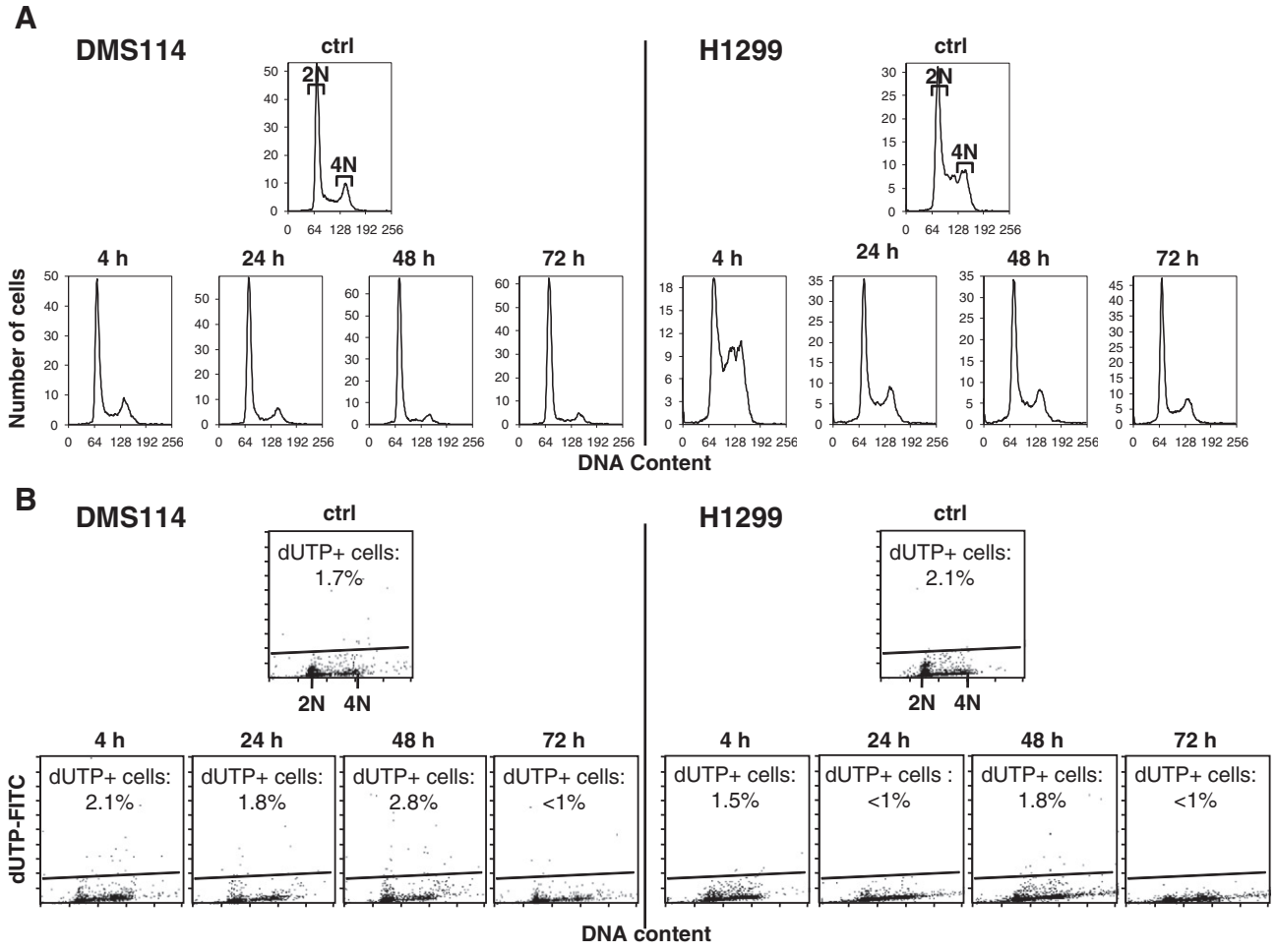

Figure 2. Cell cycle perturbation and apoptosis induced by lucitanib treatment. A. Flow cytometric analysis of DNA content during treatment with IC_{50} lucitanib dose in H1299 cells (right panel, 10 μM) and DMS114 cells (left panel, 1 μM). Upper panels show the DNA content of untreated cells ("ctrl"), while lower panels show the DNA content of cells treated with IC50 lucitanib dose for 4, 24, 48 and 72 hours. B. Flow cytometric analysis of apoptotic cells represented by biparametric PI fluorescence (DNA content) and dUTP-FITC fluorescence. Untreated and treated cells are represented as in Panel *A* at the same times and doses of treatment. Cells with DNA fragmentation induced during apoptosis are dUTP-positive (above the straight line). DNA corresponding to G_1 (2 N) and G_2 M (4 N) cells is indicated.

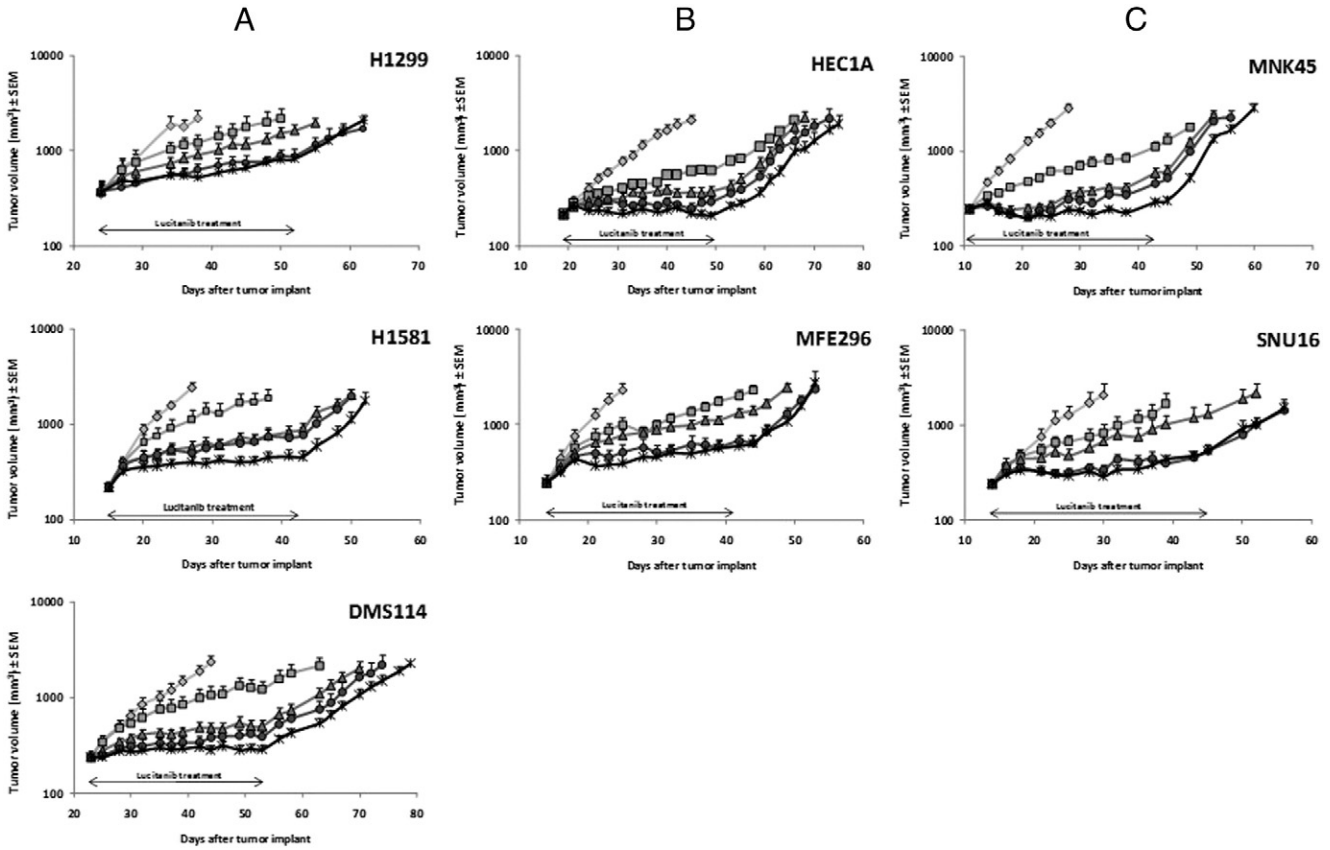

Figure 3. Lucitanib *in vivo* antitumor activity in aberrant and wt *FGFR1* or *FGFR2* lung, endometrial and gastric cancer xenografts. A Inhibition of the growth of lung tumor xenografts (upper panel: H1299 tumor xenograft (NSCLC *FGFR1* wt), middle panel: H1581 tumor xenograft (NSCLC *FGFR1* amplified), lower panel: DSM114 xenograft (SCLC *FGFR1* amplified); B Inhibition of the growth of endometrial tumor xenografts (upper panel: HEC1A *FGFR2* wt; lower panel: MFE296 (*FGFR2 N550 K*); C. Inhibition of the growth of gastric tumor xenografts (upper panel: MNK45 *FGFR2* wt; lower panel: SNU16 *FGFR2* amplified).The different xenografts were subcutaneously transplanted into nude mice as described in Material and Methods. When tumor volumes reached 200–250 mm^3, mice were randomized to receive vehicle (□) or 2.5 (■), 5 (▲), 10 (●) and 20 (*) mg/kg lucitanib doses administered orally, daily for 30 days. Arithmetic mean tumor volumes (+/− SEM) of 8–10 animals per group are shown.

FGFR2 amplified or mutated cancer cell lines were markedly more sensitive to lucitanib treatment (IC_{50}s of 0.045–3.16 μM) than the respective tumor type cell lines with wt *FGFR1* and wt *FGFR2* (IC_{50}s of 3–23 μM) (Figure 1). In lung cancer cell lines, lower IC_{50} values were associated with higher FGFR1 gene copy number (Supplementary Figure 1*B*).

Perturbation of the cell cycle was investigated in *FGFR1* amplified (DMS114) and non-amplified (H1299) cell lines by treating cells with corresponding lucitanib IC_{50} (1 μM and 10 μM respectively) for 4, 24, 48 and 72 hours. A G1 block starting at 24 hours and persisting up to 48 hours of treatment was observed in DMS114 cells, while a clear late S-G2/M blockade of the cell cycle in H1299 cells was observed (Figure 2, upper panel A). Both effects were more evident at twice the IC_{50} dose (data not shown). In the same experimental conditions, no apoptosis was detected by TUNEL assay (Figure 2*B*, lower panel), suggesting a cytostatic, rather than cytotoxic, effect of drug treatment in both the *FGFR1* amplified and non-amplified cells used here. Modulation of the FGFR1 pathway signaling was investigated *in vitro*. As shown in Supplementary Figure 2, a decrease in FGFR, FRS2 and ERK phosphorylation was observed in both H1581 and SNU16 cells after 2 hours of lucitanib treatment ≥100 nM.

Lucitanib Inhibits In Vivo Tumor Growth in Lung, Gastric and Endometrial Carcinoma Xenograft Models

The antitumor activity of lucitanib was evaluated in mice subcutaneously implanted with *FGFR1/2* gene amplified (n = 3) and non-amplified cell lines (n = 2). Mice with established tumors were treated with 2.5, 5, 10 or 20 mg/kg QD lucitanib PO. Dose-dependent antitumor activity was observed in all the xenograft models (Figure 3), with a greater antitumor activity at higher doses (Figure 3 and Table 2). At the lowest dose tested (2.5 mg/kg) partial inhibition of tumor growth was observed in all models.

In lung xenograft models, lucitanib was preferentially active in the two *FGFR1* amplified models than in the non-amplified model (Figure 3*A* and Table 2). At the 5 mg/kg dose, in H1299 non-amplified *FGFR1* xenografts, lucitanib was less active than in the H1581 and DMS114 amplified *FGFR1* xenografts, with T/C values of 41% (H1299) compared to 24% (H1581) and 20% (DMS114). The antitumor activities at 5 mg/kg for *FGFR1*-amplified models were comparable with those observed at the higher doses 10 and 20 mg/kg in the *FGFR1* non-amplified model (Figure 3*A* and Table 2). No tumor regressions were observed in any of the lung xenograft models tested at any dose schedule, with the best effect observed being tumor stabilization.

Table 2. *In vivo* Antitumor Activity of Lucitanib in the Different Xenograft Models

Tumor (Type)	*FGFR* Status	Lucitanib Dose (mg/kg)	Best T/C% (Day After Implant)
Lung Carcinoma			
H1299 (NSCLC)	*FGFR1* wt	2.5	55 (38)
		5	41 (38)
		10	28 (38)
		20	24 (38)
H1581 (NSCLC)	*FGFR1* amplified	2.5	46 (27)
		5	24 (27)
		10	21 (27)
		20	16 (27)
DMS114 (SCLC)	*FGFR1* amplified	2.5	45 (44)
		5	20 (46)
		10	16 (44)
		20	12 (44)
Gastric Carcinoma			
MNK45	*FGFR2* wt	2.5	22 (28)
		5	12 (28)
		10	10 (32)
		20	7 (32)
SNU16	*FGFR2* amplified	2.5	40 (30)
		5	32 (30)
		10	16 (30)
		20	14 (30)
Endometrial Carcinoma			
HEC1A	*FGFR2* wt	2.5	29 (45)
		5	17 (47)
		10	12 (45)
		20	10 (49)
MFE296	*FGFR2* mutated	2.5	36 (28)
		5	34 (25)
		10	22 (30)
		20	17 (25)

Best T/C% values were calculated as described in Materials and Methods.

In gastric and endometrial cancer models, lucitanib treatment caused a dose-dependent tumor growth inhibition in all xenografts. The antitumor activity observed in *FGFR2* non-amplified gastric xenograft model (MNK45) was comparable to the one in the one *FGFR2* amplified (SNU16) (Figure 3*C* and Table 2). Similarly, lucitanib exerted a dose-dependent antitumor activity in endometrial cancer xenografts models regardless of FGFR2 mutational status (Figure 3*B*, and Table 2). Tumor regressions were observed at the highest tested dose of 20 mg/kg in HEC1A and MNK45 bearing wt *FGFR2*, in 2 and 3 out of 10 mice respectively (data not shown).

Lucitanib Pharmacokinetics After Chronic Drug Treatment

To better characterize the pharmacological properties of lucitanib, mice bearing H1299, H1581 and DMS114 lung xenografts were treated for 12 consecutive days with different doses of lucitanib. Twelve days of continuous drug treatment was predicted to achieve the steady-state plasma concentration based on previous studies (35, 36). At 4 (Figure 4, *A* and *B*) and 24 hours (Figure 4, *C* and *D*) after the last administered dose, animals were sacrificed and drug concentrations were measured in plasma and tumors. At both time points, lucitanib concentrations were similar in the different tumor models (Supplementary Table 1), were correlated to the administered dose (Figure 4). No difference in drug levels was observed in regards to *FGFR1* amplification status (Supplementary Table 1). The drug accumulated in tumors after repeated treatments, with tumor/plasma ratios increasing from 2.5 ± 0.7 at 4 hours to 24.8 ± 7.4 at 24 hours. Comparable plasma and tumor drug levels were found in the endometrial and gastric xenograft models (Supplementary Figure 3).

Discussion

Lucitanib is a novel small molecule that selectively binds VEGFR1–3, PDGFRα/β and FGFR1–3 receptor tyrosine kinases with Kd <100 nM in biochemical assays. Our previous data have shown that lucitanib is highly active as a single agent in diverse human tumor xenografts with antitumor activity being related to its anti-angiogenic effects [34]. In addition, a synergistic effect of the combination lucitanib plus paclitaxel was demonstrated in triple negative breast cancer human xenografts [35]. In the present study, we explored the ability of lucitanib to inhibit the FGFR pathway in different experimental systems characterized by deregulation of the pathway due to increased levels of FGFR1/2 mRNA, amplified *FGFR1*, and/or expression of mutated or amplified *FGFR2*.

Although FGFR1 has been identified as a potential driver for cell proliferation in breast and lung cancer cell lines [36,37], it remains to be established whether *FGFR1* gene copy number is a predictive biomarker for response to FGFR1 inhibition in terms of tumor growth and survival. Data reported on NSCLC cells suggest that *FGFR1* amplification does not always predict sensitivity to FGFR1 inhibition [15]. Only the H1581 cell line, harboring a focal *FGFR1* amplification, was growth-inhibited when treated with shRNA targeting FGFR1. An association between *FGFR1* amplification and response to NVP-BGJ398, a selective pan-FGFR inhibitor, was found when a large panel of cell lines were tested [27]. However, in the same study, 54% of the over-expressing *FGFR1* mRNA cell lines were not sensitive to the drug suggesting that additional genetic alterations may play a role in FGFR dependency [27]. *FGFR1* mRNA was shown to be a better biomarker for ponatinib response in lung cancer than *FGFR1* gene copy number [38]. A discrepancy between FGFR1 amplification level and FGFR1 protein expression was reported in a panel of lung cell lines, and low FGFR1 expression was associated with resistance to the different FGFR inhibitors [39]. In the panel of cell lines used in the present study, we found an *in vitro* correlation between *FGFR1* gene copy number and *FGFR1* mRNA, and showed that lucitanib inhibition of cellular proliferation was higher in lung cancer cells harboring the higher *FGFR1* gene copies. Lucitanib mainly induced cytostatic effect in the *FGFR1*-aberrant DMS114 SCLC cell line. Drug treatment of these cells caused a clear G1 block and no induction of apoptosis. In the H1299 NSCLC cell line, wt for *FGFR1*, a late S-G2 block and no induction of apoptosis was observed, suggesting a different cytostatic mechanism. Lucitanib was also extremely active in *FGFR2* amplified or mutated cell lines with a 10-fold lower drug IC_{50} than in *FGFR2* wt cells.

The marked activity of lucitanib *in vitro* in cells where the *FGFR1/2* pathway is aberrant is consistent with the activity reported in preclinical models for other anti-FGFR compounds [24,40]. However for lucitanib, the translation of this antitumor effect *in vivo* is complicated by the fact that the drug has a more potent inhibitory activity on VEGFRs/PDGFRs than FGFRs [34,35] and that the VEGFRs have a direct role in tumor angiogenesis. In order to dissect the relative contribution of the inhibition of these receptors (VEGFRs and FGFRs) to the antitumor activity of lucitanib, the compound was tested at a range of doses in wt and *FGFR1* amplified lung cancer cells, in wt and mutated *FGFR2* endometrial cancer cells and in wt and *FGFR2* amplified gastric cancer cells transplanted subcutaneously into nude mice. Lucitanib showed a dose dependent antitumor activity, with activity observed even at the lowest dose tested (2.5 mg/kg). In *FGFR1* amplified xenografts lucitanib had greater antitumor activity as compared to *FGFR1* wt xenograft, especially at the 5 mg/kg dose.

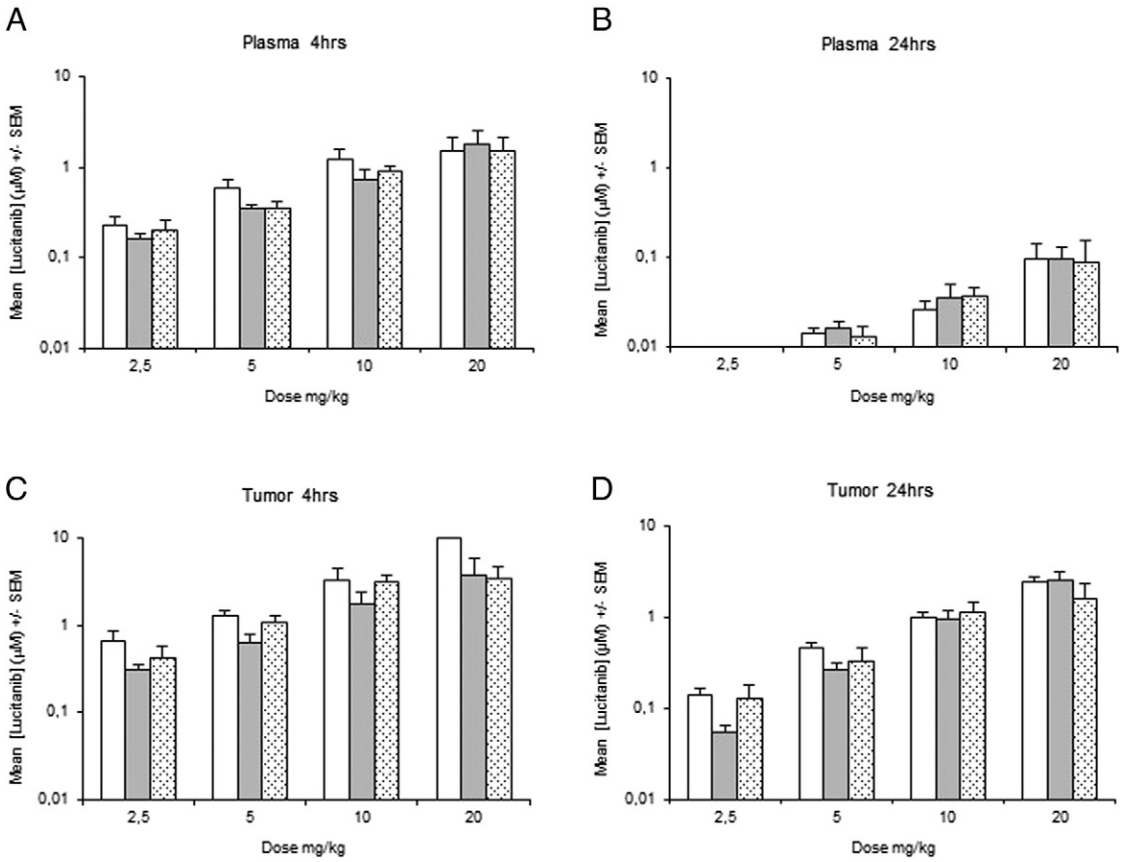

Figure 4. Lucitanib plasma (A) and tumor (B) concentrations in lung xenografts. The different xenografts were subcutaneously transplanted into nude mice and when tumor volumes reached 300–400 mg, mice were daily treated for 12 days at the indicated doses. 4 hours (right panels A and B) and 24 hours (left panels A and B) after the last drug administration, animals were sacrificed and plasma and tumors taken. Drug levels were determined as specified in Materials and Methods. The mean of lucitanib concentration + SD of four different animals are shown, for mice bearing H1299 (□; H1581 (■); DMS114 (⧈) xenografts, respectively.

Pharmacokinetic analysis clearly showed that lucitanib tumor levels at 4 and 24 hours after the last dose intake following 12 days treatment were correlated to the administered dose and were comparable in wt (H1299) and amplified *FGFR1* (H1581 and DMS114) xenografts. Tumor drug concentrations at 4 hours were similar to the *in vitro* IC_{50} values for *FGFR1* wt H1299, but much higher (from 3 to 26 fold) than the IC_{50} values for *FGFR1* amplified H1581 and DMS114 tumors. Interestingly, the drug accumulated in the tumor with high tumor/plasma ratios that increased with time from 2.5 at 4 hours to 24.8 at 24 hours post-dosing. In agreement with these data, a high lucitanib tumor distribution has recently been reported in a breast cancer biopsy from a woman participating in the First in Human Study of lucitanib. After 21 days of treatment, just before the daily oral dose of 10 mg, lucitanib achieved a tumor drug concentration of 11 µM, 25 fold higher than the concomitant plasma drug concentration of 0.43 µM [33]. This clinical data and the preclinical data presented herein would suggest a high accumulation of the drug in the tumor.

Lucitanib was preferentially cytostatic *in vitro* in *FGFR2* amplified and mutated cell lines as opposed to in cell lines where FGFR2 was wild-type (Figure 1). However, the *in vivo* effect of lucitanib on tumor growth in all endometrial and gastric cancer xenograft models studied was similar, regardless of *FGFR2* status. In particular, some tumor regressions were seen in wt *FGFR2* endometrial and gastric xenograft models at the highest dose of lucitanib (20 mg/kg). Thus, in these models, the potent anti-angiogenic activity of lucitanib likely masked the effect of inhibiting FGFR2 signaling in the tumor cells.

In conclusion, the current study provides evidence that lucitanib is able to potently inhibit the FGF/FGFR pathway and FGFR-dependent tumor cell proliferation *in vitro*. Our *in vivo* data in *FGFR1* deregulated systems suggest that simultaneous inhibition of VEGF and FGF receptors in *FGFR1* dependent tumors can be therapeutically advantageous. Interestingly, while lucitanib showed enhanced inhibition of *FGFR1* amplified lung xenografts, lucitanib was highly active in all endometrial and gastric xenografts models tested, irrespective of *FGFR2* status. The role of FGFR aberrations as a predictive biomarker for response to lucitanib should be further evaluated and validated in prospective clinical studies.

Supplementary data to this article can be found online at http://dx.doi.org/10.1016/j.neo.2016.11.008.

Acknowledgements

This research was supported by a research grant from Servier. We thank Céline Bossard‡ and Carine Saunier‡ for performing the western-blot assays.

References

[1] Turner N and Grose R (2010). Fibroblast growth factor signalling: from development to cancer. *Nat Rev Cancer* **10**, 116–129.

[2] Lieu C, Heymach J, Overman M, Tran H, and Kopetz S (2011). Beyond VEGF: inhibition of the fibroblast growth factor pathway and antiangiogenesis. *Clin Cancer Res* **17**, 6130–6139.

[3] Crawford Y and Ferrara N (2009). Tumor and stromal pathways mediating refractoriness/resistance to anti-angiogenic therapies. *Trends Pharmacol Sci* **30**, 624–630.

[4] Dieci MV, Arnedos M, Andre F, and Soria JC (2013). Fibroblast growth factor receptor inhibitors as a cancer treatment: from a biologic rationale to medical perspectives. *Cancer Discov* **3**, 264–279.

[5] Wesche J, Haglund K, and Haugsten EM (2011). Fibroblast growth factors and their receptors in cancer. *Biochem J* **437**, 199–213.

[6] Dienstmann R, Rodon J, Prat A, Perez-Garcia J, Adamo B, Felip E, Cortes J, Iafrate AJ, Nuciforo P, and Tabernero J (2014). Genomic aberrations in the FGFR pathway: opportunities for targeted therapies in solid tumors. *Ann Oncol* **25**, 552–563.

[7] Parker BC, Engels M, Annala M, and Zhang W (2014). Emergence of FGFR family gene fusions as therapeutic targets in a wide spectrum of solid tumours. *J Pathol* **232**, 4–15.

[8] Wu YM, F S, Kalyana-Sundaram S, Khazanov N, Ateeq B, Cao X, Lonigro RJ, Vats P, Wang R, and Lin SF, et al (2013). Identification of targetable FGFR gene fusions in diverse cancers. *Cancer Discov* **3**, 636–647.

[9] Brooks AN, Kilgour E, and Smith PD (2012). Molecular pathways: fibroblast growth factor signaling: a new therapeutic opportunity in cancer. *Clin Cancer Res* **18**, 1855–1862.

[10] Heinzle C, Sutterluty H, Grusch M, Grasl-Kraupp B, Berger W, and Marian B (2011). Targeting fibroblast-growth-factor-receptor-dependent signaling for cancer therapy. *Expert Opin Ther Targets* **15**, 829–846.

[11] Reis-Filho JS, Simpson PT, Turner NC, Lambros MB, Jones C, Mackay A, Grigoriadis A, Sarrio D, Savage K, and Dexter T, et al (2006). FGFR1 emerges as a potential therapeutic target for lobular breast carcinomas. *Clin Cancer Res* **12**, 6652–6662.

[12] Turner N, Pearson A, Sharpe R, Lambros M, Geyer F, Lopez-Garcia MA, Natrajan R, Marchio C, Iorns E, and Mackay A, et al (2010). FGFR1 amplification drives endocrine therapy resistance and is a therapeutic target in breast cancer. *Cancer Res* **70**, 2085–2094.

[13] *Comprehensive molecular profiling of lung adenocarcinomaNature* **511**, 543–550.

[14] Cihoric N, Savic S, Schneider S, Ackermann I, Bichsel-Naef M, Schmid RA, Lardinois D, Gugger M, Bubendorf L, and Zlobec I, et al (2014). Prognostic role of FGFR1 amplification in early-stage non-small cell lung cancer. *Br J Cancer* **110**, 2914–2922.

[15] Dutt A, Ramos AH, Hammerman PS, Mermel C, Cho J, Sharifnia T, Chande A, Tanaka KE, Stransky N, and Greulich H, et al (2011). Inhibitor-sensitive FGFR1 amplification in human non-small cell lung cancer. *PLoS One* **6**, e20351.

[16] Matsumoto K, Arao T, Hamaguchi T, Shimada Y, Kato K, Oda I, Taniguchi H, Koizumi F, Yanagihara K, and Sasaki H, et al (2012). FGFR2 gene amplification and clinicopathological features in gastric cancer. *Br J Cancer* **106**, 727–732.

[17] Al-Ahmadie HA, Iyer G, Janakiraman M, Lin O, Heguy A, Tickoo SK, Fine SW, Gopalan A, Chen YB, and Balar A, et al (2011). Somatic mutation of fibroblast growth factor receptor-3 (FGFR3) defines a distinct morphological subtype of high-grade urothelial carcinoma. *J Pathol* **224**, 270–279.

[18] Tomlinson DC, Baldo O, Harnden P, and Knowles MA (2007). FGFR3 protein expression and its relationship to mutation status and prognostic variables in bladder cancer. *J Pathol* **213**, 91–98.

[19] Capdevila J, Carrato A, Tabernero J, and Grande E (2014). What could Nintedanib (BIBF 1120), a triple inhibitor of VEGFR, PDGFR, and FGFR, add to the current treatment options for patients with metastatic colorectal cancer? *Crit Rev Oncol Hematol* **92**, 83–106.

[20] Chou T and Finn RS (2012). Brivanib: a review of development. *Future Oncol* **8**, 1083–1090.

[21] Andre F, Bachelot T, Campone M, Dalenc F, Perez-Garcia JM, Hurvitz SA, Turner N, Rugo H, Smith JW, and Deudon S, et al (2013). Targeting FGFR with dovitinib (TKI258): preclinical and clinical data in breast cancer. *Clin Cancer Res* **19**, 3693–3702.

[22] Konecny GE, Kolarova T, O'Brien NA, Winterhoff B, Yang G, Qi J, Qi Z, Venkatesan N, Ayala R, and Luo T, et al (2013). Activity of the fibroblast growth factor receptor inhibitors dovitinib (TKI258) and NVP-BGJ398 in human endometrial cancer cells. *Mol Cancer Ther* **12**, 632–642.

[23] Gozgit JM, Wong MJ, Moran L, Wardwell S, Mohemmad QK, Narasimhan NI, Shakespeare WC, Wang F, Clackson T, and Rivera VM (2012). Ponatinib (AP24534), a multitargeted pan-FGFR inhibitor with activity in multiple FGFR-amplified or mutated cancer models. *Mol Cancer Ther* **11**, 690–699.

[24] Gavine PR, Mooney L, Kilgour E, Thomas AP, Al-Kadhimi K, Beck S, Rooney C, Coleman T, Baker D, and Mellor MJ, et al (2012). AZD4547: an orally bioavailable, potent, and selective inhibitor of the fibroblast growth factor receptor tyrosine kinase family. *Cancer Res* **72**, 2045–2056.

[25] Zhang J, Zhang L, Su X, Li M, Xie L, Malchers F, Fan S, Yin X, Xu Y, and Liu K, et al (2012). Translating the therapeutic potential of AZD4547 in FGFR1-amplified non-small cell lung cancer through the use of patient-derived tumor xenograft models. *Clin Cancer Res* **18**, 6658–6667.

[26] Zhao G, Li WY, Chen D, Henry JR, Li HY, Chen Z, Zia-Ebrahimi M, Bloem L, Zhai Y, and Huss K, et al (2011). A novel, selective inhibitor of fibroblast growth factor receptors that shows a potent broad spectrum of antitumor activity in several tumor xenograft models. *Mol Cancer Ther* **10**, 2200–2210.

[27] Guagnano V, Kauffmann A, Wohrle S, Stamm C, Ito M, Barys L, Pornon A, Yao Y, Li F, and Zhang Y, et al (2012). FGFR genetic alterations predict for sensitivity to NVP-BGJ398, a selective pan-FGFR inhibitor. *Cancer Discov* **2**, 1118–1133.

[28] Tabernero J, Bahleda R, Dienstmann R, Infante JR, Mita A, Italiano A, Calvo E, Moreno V, Adamo B, and Gazzah A, et al (2015). Phase I Dose-Escalation Study of JNJ-42756493, an Oral Pan-Fibroblast Growth Factor Receptor Inhibitor, in Patients With Advanced Solid Tumors. *J Clin Oncol* **33**, 3401–3408.

[29] Andre F, Daly F, Azim Jr HA, Agrapart V, Fumagalli D, Gingras I, Guitart M, Lange A, Turner NC, and Pierrat M-J, et al (2015). FINESSE - An open, 3-cohort, phase II trial testing oral administration of lucitanib in patients with FGFR1-amplified or non-amplIfied oestrogeN rEceptor poSitive metaStatic breast cancEr. San Antonio Breast Cancer Symposium - December 8–12, 2015; 2015.

[30] Soria JC, DeBraud F, Bahleda R, Adamo B, Andre F, Dientsmann R, Delmonte A, Cereda R, Isaacson J, and Litten J, et al (2014). Phase I/IIa study evaluating the safety, efficacy, pharmacokinetics, and pharmacodynamics of lucitanib in advanced solid tumors. *Ann Oncol* **25**, 2244–2251.

[31] Burbridge MF, Bossard CJ, Saunier C, Fejes I, Bruno A, Leonce S, Ferry G, Da Violante G, Bouzom F, and Cattan V, et al (2013). S49076 is a novel kinase inhibitor of MET, AXL, and FGFR with strong preclinical activity alone and in association with bevacizumab. *Mol Cancer Ther* **12**, 1749–1762.

[32] Sala F, Bagnati R, Livi V, Cereda R, D'Incalci M, and Zucchetti M (2011). Development and validation of a high-performance liquid chromatography–tandem mass spectrometry method for the determination of the novel inhibitor of angiogenesis E-3810 in human plasma and its application in a clinical pharmacokinetic study. *J Mass Spectrom* **46**, 1039–1045.

[33] Zangarini M, Ceriani L, Bello E, Damia G, Cereda R, Camboni MG, and Zucchetti M (2014). HPLC-MS/MS method for quantitative determination of the novel dual inhibitor of FGF and VEGF receptors E-3810 in tumor tissues from xenograft mice and human biopsies. *J Mass Spectrom* **49**, 19–26.

[34] Bello E, Colella G, Scarlato V, Oliva P, Berndt A, Valbusa G, Serra SC, D'Incalci M, Cavalletti E, and Giavazzi R, et al (2011). E-3810 is a potent dual inhibitor of VEGFR and FGFR that exerts antitumor activity in multiple preclinical models. *Cancer Res* **71**, 1396–1405.

[35] Bello E, Taraboletti G, Colella G, Zucchetti M, Forestieri D, Licandro SA, Berndt A, Richter P, D'Incalci M, and Cavalletti E, et al (2013). The tyrosine kinase inhibitor E-3810 combined with paclitaxel inhibits the growth of advanced-stage triple-negative breast cancer xenografts. *Mol Cancer Ther* **12**, 131–140.

[36] Turner N, Lambros MB, Horlings HM, Pearson A, Sharpe R, Natrajan R, Geyer FC, van Kouwenhove M, Kreike B, and Mackay A, et al (2010). Integrative molecular profiling of triple negative breast cancers identifies amplicon drivers and potential therapeutic targets. *Oncogene* **29**, 2013–2023.

[37] Weiss J, Sos ML, Seidel D, Peifer M, Zander T, Heuckmann JM, Ullrich RT, Menon R, Maier S, and Soltermann A, et al (2010). Frequent and focal FGFR1 amplification associates with therapeutically tractable FGFR1 dependency in squamous cell lung cancer. *Sci Transl Med* **2**, 62ra93.

[38] Wynes MW, Hinz TK, Gao D, Martini M, Marek LA, Ware KE, Edwards MG, Bohm D, Perner S, and Helfrich BA, et al (2014). FGFR1 mRNA and protein expression, not gene copy number, predict FGFR TKI sensitivity across all lung cancer histologies. *Clin Cancer Res* **20**, 3299–3309.

[39] Kotani H, Ebi H, Kitai H, Nanjo S, Kita K, Huynh TG, Ooi A, Faber AC, Mino-Kenudson M, and Yano S (2016). Co-active receptor tyrosine kinases mitigate the effect of FGFR inhibitors in FGFR1-amplified lung cancers with low FGFR1 protein expression. *Oncogene* **35**, 3587–3597.

[40] Guagnano V, Furet P, Spanka C, Bordas V, Le Douget M, Stamm C, Brueggen J, Jensen MR, Schnell C, and Schmid H, et al (2011). Discovery of 3-(2,6-dichloro-3,5-dimethoxy-phenyl)-1-{6-[4-(4-ethyl-piperazin-1-yl)-phenylamin o]-pyrimidin-4-yl}-1-methyl-urea (NVP-BGJ398), a potent and selective inhibitor of the fibroblast growth factor receptor family of receptor tyrosine kinase. *J Med Chem* **54**, 7066–7083.